

Biomimetics | Hot Paper |

 Photoinduced Charge Transfer in a Conformational Switching Chlorin Dimer–Azafulleroid in Polar and Nonpolar MediaTaru Nikkonen,^[a] María Moreno Oliva,^[b] Axel Kahnt,^{*,[b]} Mikko Muuronen,^[a] Juho Helaja,^{*,[a]} and Dirk M. Guldi^{*,[b]}

Abstract: In the present study, a biomimetic reaction center model, that is, a molecular triad consisting of a chlorin dimer and an azafulleroid, is synthesized and its photophysical properties are studied in comparison with the corresponding molecular dyad, which consists only of a chlorin monomer and an azafulleroid. As evidenced by ¹H NMR, UV/Vis, and fluorescence spectroscopy, the chlorin dimer–azafulleroid folds in nonpolar media into a C₂-symmetric geometry through hydrogen bonding, resulting in appreciable electronic interactions between the chlorins, whereas in polar media the two chlorins diverge from contact. Femtosecond transient absorption spectroscopy studies reveal longer charge-separated states for the chlorin dimer–azafulleroid; ≈ 1.6 ns in toluene, compared with the lifetime of ≈ 0.9 ns for the corresponding chlorin monomer–azafulleroid in toluene. In polar media, for example, benzonitrile, similar charge-separated states are observed, but the lifetimes are inevitably shorter: 65 and 73 ps for the dimeric and monomeric chlorin–azafulleroids, respectively. Nanosecond transient absorption and singlet oxygen phosphorescence

studies corroborate that in toluene, the charge-separated state decays indirectly via the triplet excited state to the ground state, whereas in benzonitrile, direct recombination to the ground state is observed. Complementary DFT studies suggest two energy-minima conformations, that is, a folded chlorin dimer–azafulleroid, which is present in nonpolar media, and another conformation in polar media, in which the two hydrophobic chlorins wrap the azafulleroid. Inspection of the frontier molecular orbitals shows that in the folded conformation, the HOMO on each chlorin is equivalent and is shared owing to partial π–π overlap, resulting in delocalization of the conjugated π electrons, whereas the wrapped conformation lacks this stabilization. As such, the longer charge-separated lifetime for the dimer is rationalized by both the electron donor–acceptor separation distance and the stabilization of the radical cation through delocalization. The chlorin folding seems to change the photophysical properties in a manner similar to that observed in the chlorophyll dimer in natural photosynthetic reaction centers.

Introduction

In the photosynthetic systems of green plants and algae, chlorophylls (Chls) and bacteriochlorophylls (BChls) function in variable roles to convert light energy efficiently into chemical energy. Depending on the environment and the distance of a (B)Chl from the neighboring chlorophyll of one and the same

unit, it may undergo light absorption, excitation energy transfer, and/or charge separation.^[1]


To adapt to divergent environments, nature has developed different assemblies of photosynthetic systems to produce charges from light with the utmost efficiency. In particular, light-harvesting antennae assemblies, responsible for excitation energy transfer, have broad structural diversity. In contrast, the study of primary electron-transfer events in various photosynthetic reaction centers has revealed similarities in terms of the initial charge separation and the subsequent charge shift in those systems that utilize a dimeric Chl as a primary electron donor.^[2] This dimer is commonly known as a Chl special pair (SP). Characteristically, it exhibits a C₂ symmetry consisting of two intermolecularly assembled Chls, which are in close proximity with a partial π–π overlap. Unambiguously, such an assembly enables strong interactions between the HOMOs, creating a shared “supermolecular” HOMO for the SP.^[3] On one hand, this feature renders the SP prone to fast and efficient photoinduced oxidation, namely, charge separation. On the other hand, the reverse pathway, that is, charge recombination, inevitably slows down and does not occur in the natural environment. In short, direct photoexcitation or excitation energy

[a] T. Nikkonen,⁺ M. Muuronen, Dr. J. Helaja

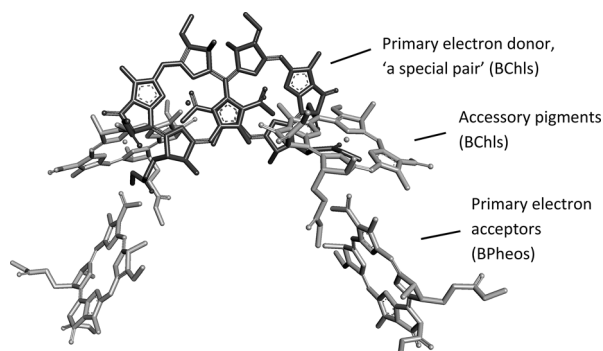
Department of Chemistry
Laboratory of Organic Chemistry
University of Helsinki
P. O. Box 55,00014, University of Helsinki (Finland)
E-mail: juho.helaja@helsinki.fi

[b] Dr. M. M. Oliva,⁺ Dr. A. Kahnt, Prof. Dr. D. M. Guldi
Department of Chemistry and Pharmacy & Interdisciplinary Center for Molecular Materials (ICMM)
Friedrich-Alexander-Universität Erlangen-Nürnberg
Egerlandstraße 3, 91058 Erlangen (Germany)
E-mail: axel.kahnt@fau.de
dirk.guldi@fau.de

[⁺] These authors contributed equally to this work.

 Supporting information for this article is available on the WWW under <http://dx.doi.org/10.1002/chem.201404786>.

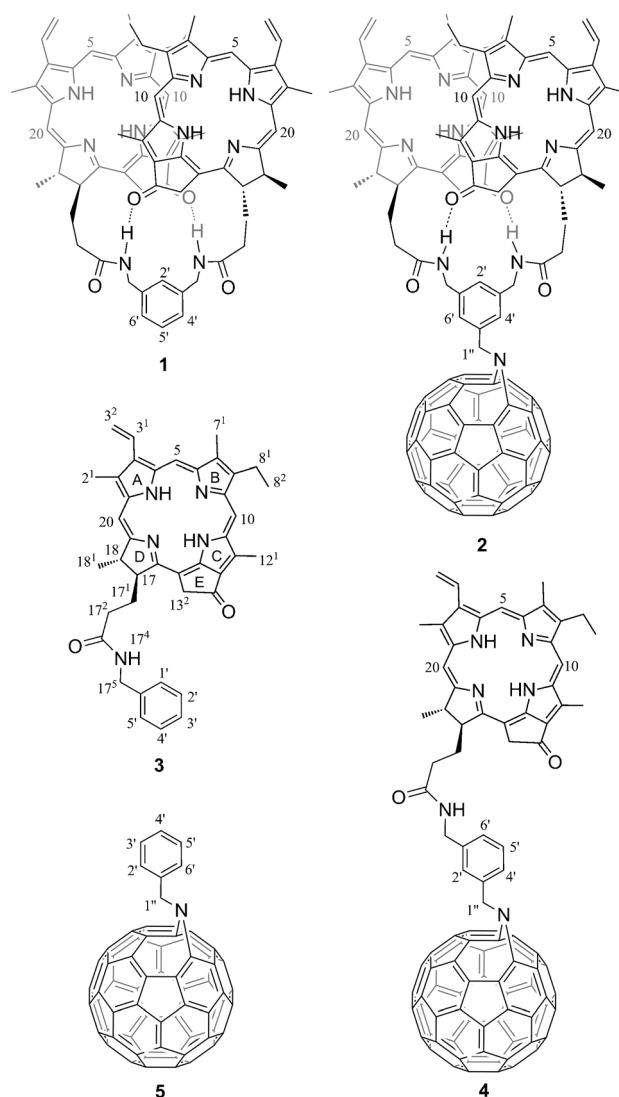
transfer from the antennae leads to excitation and subsequent oxidation to afford SP^+ , which possesses an equally delocalized radical cation. Subsequently, the electron is transferred to electron acceptors of the electron-transfer cycle. In this cycle, electrons flow, and the positive charge at SP^+ is balanced by an electron. The structure of the natural reaction center of *Rhodospseudomonas viridis* utilizing dimeric BChl as a primary electron donor is shown in Scheme 1.^[4]



Scheme 1. The pigment organization in the photosynthetic reaction center of *Rhodospseudomonas viridis*, in which the dark gray BChl dimer forms the “special pair”.^[4]

Several groups have been inspired to design and probe artificial mimics of photosynthetic reaction centers. The common feature for most of the corresponding systems is that monomeric electron donors such as chlorins,^[5] porphyrins,^[6] or phthalocyanines^[6a-c,7] have been attached either covalently or noncovalently to electron acceptors such as fullerenes, carbon nanotubes, and so on. Models with biomimetic SPs are rare, and are limited to a few studies.^[8] In these charge-transfer models, the SP is often constructed from porphyrins^[8b-k] or phthalocyanines.^[8a] Despite the fact that a number of reaction centers mimicking chlorin dimers have been reported,^[9] only a handful of self-assembling chlorin dimers combined with electron acceptors have been described.^[10] The self-assembly strategy in biomimetic reaction center SP dimers is often based on the tendency of Chls to self-aggregate in the presence of external bridges such as water or alcohol.^[9,10]

In our previous study, we demonstrated that amide-linked *pyro*-pheophorbide *a* dimers are susceptible to folding.^[11] These dimers, featuring linkages of suitable lengths, fold in nonpolar solvents through intramolecular hydrogen bonding into C_2 symmetry. Evidence for this has come from absorption, fluorescence, IR, CD, and NMR spectroscopies as well as DFT studies. Here, the two amide protons in the linkage between the two Chls act as hydrogen-bond donors, whereas the 13^1 carbonyls of the two Chls are hydrogen-bond acceptors. Notably, in the stacked assembly, the chlorins give rise to interplanar orbital interactions similar to what is known from the photosynthetic reaction center SP. In the current work, we have utilized this folding strategy to construct an electron donor–acceptor conjugate biomimetically by attaching an azafulleroid covalently to a stacked dimer to afford a triad, **2** (Scheme 2).



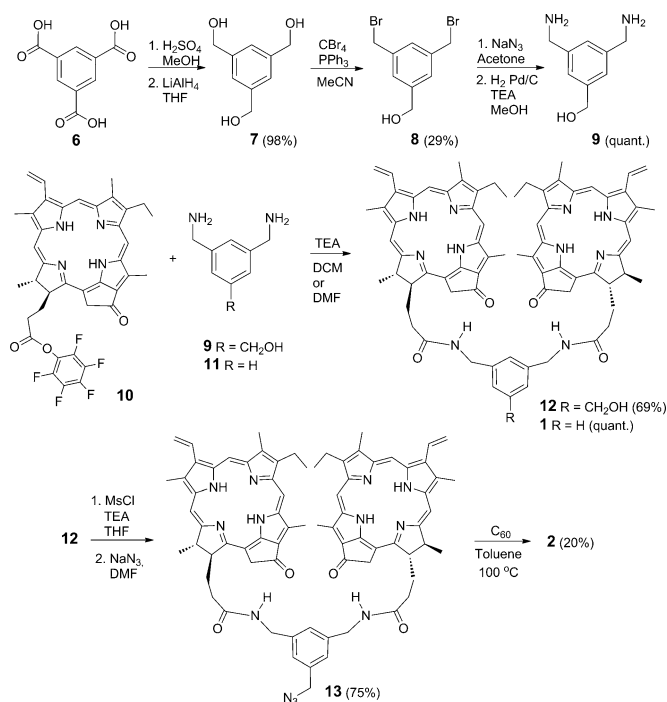
Scheme 2. Chlorin dimer **1**, chlorin dimer–azafulleroid **2**, chlorin monomer **3**, chlorin monomer–azafulleroid **4**, and benzyl azafulleroid **5**.

As the dimer, we selected a Chl dimer with a *m*-xylene linkage, **1**, which, according to our previous studies, features the optimal linker length with a five-carbon backbone and a rigid structure to ease the stacking of the two chlorins. In addition to the chlorin dimer **1** and chlorin dimer–azafulleroid **2**, the corresponding chlorin monomers **3** and **4** and the benzyl azafulleroid **5** were synthesized as references.

Results and Discussion

Synthesis

The synthesis of the studied molecules is presented in Schemes 3 and 4. Acid-catalyzed esterification of commercially available benzene-1,3,5-tricarboxylic acid **6** in methanol followed by lithium aluminum hydride reduction gave triol **7** in excellent yields.^[12] Two out of the three benzyl alcohol groups of **7** were brominated with CBr_4/PPH_3 in acetonitrile to obtain the known (3,5-bis(bromomethyl)phenyl)methanol **8** in 29%



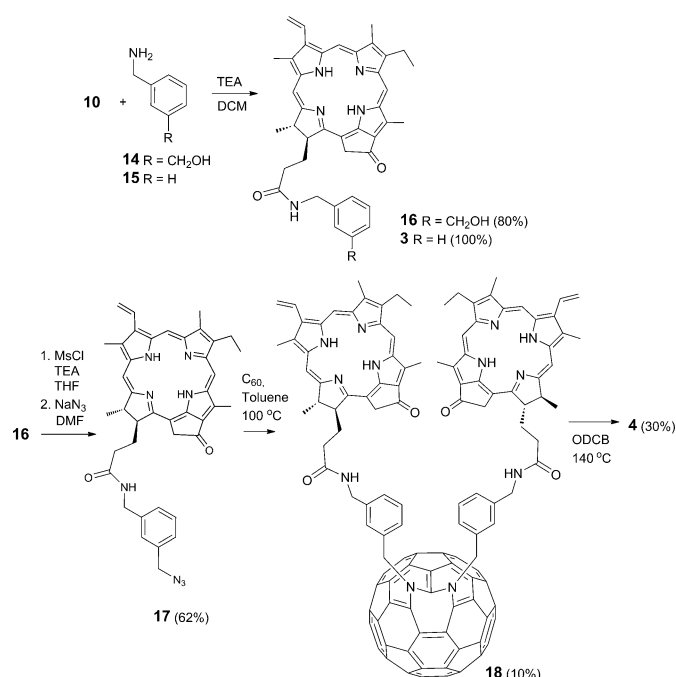
Scheme 3. Synthesis of **1** and **2** (TEA = triethylamine).

yield.^[13] Both bromines were substituted with azides by heating **8** with sodium azide in acetone and reduced by Pd/C-catalyzed hydrogenation in MeOH to afford diamine **9** in quantitative yields. Chlorin *a* was extracted from algae, *Spirulina pacifica*, and modified to give pentafluorophenol-ester-activated pyro-pheophorbide *a* (**10**), as described previously.^[11] Molecule **10** was allowed to react with diamines **9/11** to afford amide-linked pyro-pheophorbide *a* dimers **12/1**.^[11] The benzyl-alcohol-functionalized dimer **12** was treated with mesyl chloride by using a slightly modified literature procedure.^[14] The obtained mesyl derivative was relatively unstable and was allowed to react immediately with sodium azide in DMF to afford azide **13**.

The 1,3-dipolar cycloaddition (1,3-DC) of azide to the [6,6] bonds of C₆₀ followed by thermal extrusion of N₂ from the triazoline intermediate commonly leads to a mixture of two imino adducts, that is, open [5,6]-bridged azafulleroids and closed [6,6]-bridged aziridinofullerenes.^[14–19] The ratio of these two species depends on the nature of the substituent.^[15] The [6,6]-triazoline intermediates lose N₂ immediately upon heating at temperatures slightly higher than 60 °C,^[14,16,20] so this was not isolated or chemically characterized. Thermal reaction of **13** with 1.5 equivalents of C₆₀ was performed in toluene at 100 °C under argon. After stirring of the reaction mixture for 20 h, the solvent was evaporated and the crude material was purified by flash chromatography on silica gel (dichloromethane/methanol 100:1 → 10:1, gradient) to afford unreacted C₆₀ and [5,6]-open azafulleroid **2** as a main product. This was assigned by ¹H, ¹³C, COSY, NOESY, HSQC, and HMBC spectra (Figures S1–S12, Supporting Information). The HMBC spectrum of **2** displayed couplings between methylene (1'') protons at δ = 4.25 ppm and ¹³C resonance at δ_C = 144.17 ppm arising from the carbon

nucleus in C₆₀ (see magnified image in Figure S32, Supporting Information). The chemical shift of the bridging carbon atoms (δ_C = 144.17 ppm) is in the sp² region of the spectrum, and corresponds to the [5,6]-open adduct of the cycloaddition.^[15,21,22] Furthermore, the absence of ¹³C NMR signals in the range δ_C = 60–80 ppm indicates [5,6]-open adducts lacking any sp³-hybridized carbons in C₆₀.^[15]

Monomeric pyro-pheophorbide *a* (**3**) and the corresponding pyro-pheophorbide *a* with an open [5,6]-bridged azafulleroid (**4**) were synthesized in a similar fashion to dimers **1** and **2**. The starting 3-(aminomethyl)benzyl alcohol **14** was prepared from 3-cyanobenzoic acid by reduction with borane.^[23] Pentafluorophenol-ester-activated pyro-pheophorbide *a* (**10**) was allowed to react with amines **14/15** to obtain **16/3** (Scheme 4).



Scheme 4. Synthesis of **3** and **4** (Ms = methanesulfonyl, ODCB = *o*-dichlorobenzene).

Benzyl alcohol **16** was transformed into the corresponding benzyl azide **17** through the same procedure as described above for **12** to obtain **13**. Diverging from the synthesis of the chlorin dimer-azafulleroid, the reaction between the benzyl-azide-functionalized chlorin monomer **17** and C₆₀ did not afford chlorin azafulleroid **4** at 100 °C in toluene. The structure of the product was clarified by ¹H, ¹³C, COSY, NOESY, HSQC, and HMBC spectroscopy (Figures S16–S27, Supporting Information). The ¹H NMR spectrum of the product showed two sets of chlorin protons with a 1:1 measured integral ratio (Figure S22). Characteristically, in the HMBC spectrum, methylene protons (1'') of the two chlorins at δ = 4.11 and 3.76 ppm were both coupled to a carbon atom resonating at δ_C = 161.48 ppm (Figures S23, S27), which confirms the formation of bisazafulleroid **18**. The corresponding low-field chemical shift has been reported for a carbon atom adjoined to two nitrogen atoms in bisazafulleroids (diazabishomofullerenes),^[20,24] which, at times,

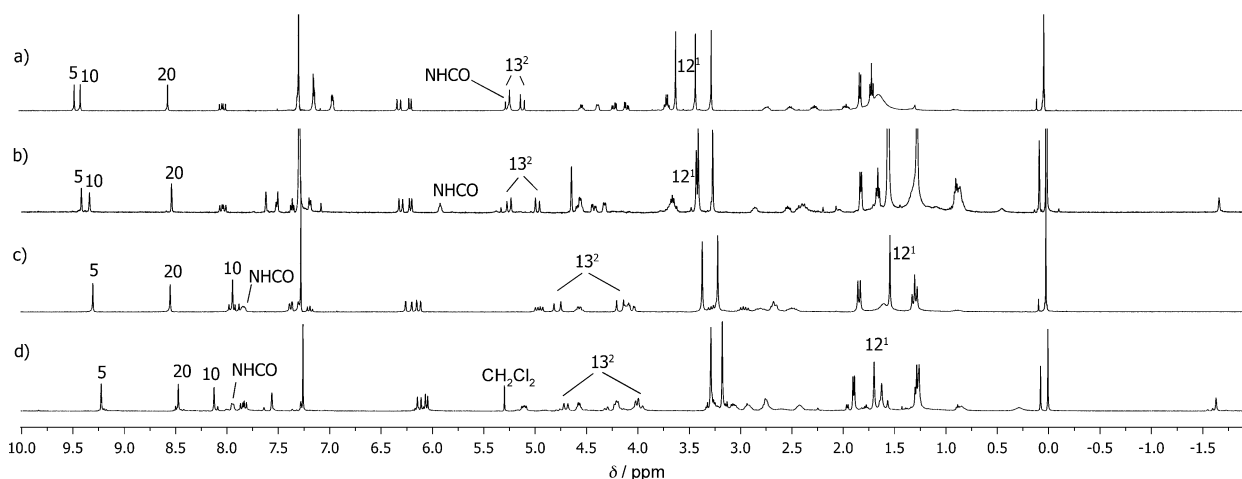


Figure 1. ^1H NMR spectra of different pyro-pheophorbide *a* derivatives (measured in CDCl_3): a) chlorin monomer **3**, b) chlorin monomer-aza fulleroid **4**, c) chlorin dimer **1**, and d) chlorin dimer-aza fulleroid **2**.

are obtained in reactions of azides with C_{60} , whereas the double bonds adjacent to the nitrogen bridge in aza fulleroids are prone to regioselective formation of bisaza fulleroids.^[24,25] Bisaza fulleroid **18** was transformed into **4** upon heating at 140°C overnight.^[24] The open [5,6]-bridged attachment was confirmed by HMBC, which showed coupling between methylene ($1''$) protons at $\delta = 4.41$ ppm and sp^2 carbon at $\delta_{\text{C}} = 145.36$ ppm (Figures S28–S31 and S33, Supporting Information).

Benzyl aza fulleroid (**5**) was prepared successfully by heating benzyl azide and C_{60} in *o*-dichlorobenzene at 160°C overnight, as described previously.^[20,21,24]

Study of intra- and intermolecular interactions

In our previous work, we observed that **1** and related chlorin dimers fold into a C_2 -symmetric geometry in nonpolar media.^[11] The folding was driven by two intramolecular hydrogen bonds between the amide as a hydrogen-bond donor and carbonyl as a hydrogen-bond acceptor (Scheme 2). The related ^1H NMR studies indicated notable shieldings for the protons that were exposed to the ring current of the neighboring macrocycle. The strongest shielded protons were H-10, H-12¹, and H-13², whereas clear deshieldings were observed for the amide protons owing to the hydrogen-bonding interactions. Comparison of the ^1H NMR spectra of **1–4** (Figure 1 a–d) reveals upfield shifts for the H-10, H-12¹, and H-13² protons in Chl dimer **1** (c) and Chl dimer-aza fulleroid **2** (d), whereas downfield shifts are measured for the amide protons. This indicates that hydrogen-bond-driven folding occurs in the chlorin dimer in nonpolar environments.

In order to break the hydrogen bonds and the folded dimer, both chlorin dimer **1** and chlorin dimer-aza fulleroid **2** were titrated with $[\text{D}_3]$ acetonitrile in CDCl_3 (Figure S34 and S35, Supporting Information). Under ^1H NMR monitoring, protons H-10 and H-12¹ are downfield shifted and amide protons (17⁴) upfield shifted during the titration. This is in accordance with the unfolding event, in which the hydrogen bonds are broken and

the two chlorins diverge from contact. During the titration experiments, chlorin dimer **1** remained soluble, but the hydrophobic chlorin dimer-aza fulleroid **2** started to precipitate gradually.

Comparing the structures of **1–4**, one can observe that monomeric chlorins **3** and **4** also contain equivalent amide and ketone groups that are capable of forming hydrogen bonds through intermolecular interactions with neighboring Chls. Furthermore, **2** and **4** feature an extra nitrogen lone pair located at the aza fulleroid, which is a potential hydrogen-bond acceptor. Analysis of the ^1H NMR spectra of **4** revealed that proton signals H-8¹, -8², -10, -12¹, -17⁴, and -1'' appeared in "unusual" spectral regions as the sample concentration was increased. Molecule **4** was diluted through stepwise addition of CDCl_3 , and the ^1H NMR spectra were taken after each dilution step (Figure S36, Supporting Information). Upon dilution, protons H-8¹, -8², -10, -12¹, and -1'' were downfield shifted, whereas the amide proton (17⁴) was upfield shifted. In other words, the "usual" chemical shifts of monomeric nonaggregated Chls were finally obtained upon dilution. This observation implies that in concentrated media, **4** forms aggregates or at least dimers, in which two or more chlorin monomer-aza fulleroids are intermolecularly locked. This interaction is probably driven by hydrogen bonds between the amide(s) and nitrogen lone pair(s) of aza fulleroid in combination with aromatic π - π interactions between Chls and C_{60} . However, these interactions are too weak to be prevailing under the diluted photophysical measurement conditions (vide infra), showing that the aggregate \leftrightarrow monomer equilibrium is clearly on the side of the monomer.

The corresponding spectral analysis of **1–3** did not indicate any intermolecular interactions under the same experimental conditions. Notably, **2** contains the same hydrogen-bond donors and acceptors as **4**, but in the former case, the formation of intramolecular hydrogen bonds to give the C_2 symmetry is entropically more favorable than intermolecular aggregation.

Photophysical studies

The absorption spectrum of chlorin monomer **3** in toluene gives rise to a strong absorption at around 415 nm, flanked by minor absorptions at 319, 510, 538, 613, and 671 nm. Here, the 415 nm band is attributed to the Soret-band absorption, whereas the bands between 500 and 700 nm are part of the Q-band absorptions. In contrast, benzyl azafulleroid **5** shows absorptions in the UV and visible regions of the solar spectrum, maximizing at 334 nm. Molecule **4** (Figure 2) exhibits ab-

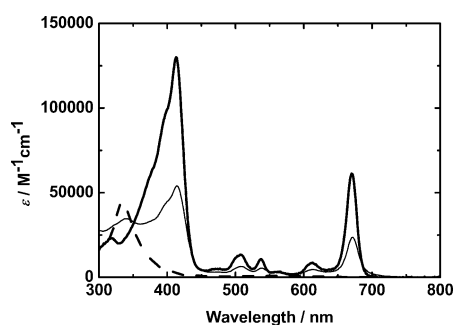


Figure 2. Absorption spectra of **4** (thin solid line) and references **3** (bold solid line) and **5** (dashed line) in toluene.

sorptions at 340, 416, 511, 540, 613, and 672 nm. As such, the absorption spectrum of **4** is best described as the superimposition of the UV/Vis spectra of reference molecules **3** and **5**. Notably, the solvent polarity has hardly any effect on the spectral features of the absorptions, as the maxima of **3** and **4** retain their positions in polar solvents such as benzonitrile. In particular, the Soret and Q_y band maxima of **3** appear at 418 and 671 nm, whereas those of **4** are seen at 419 and 672 nm (Figures S37 and S38, Supporting Information).

Turning to chlorin dimer **1**, absorptions in toluene are observed at 327, 403, 513, 544, 620, and 679 nm (Figure 3). However, unlike monomer **3**, appreciable changes are discernable upon dissolution in benzonitrile. To this end, the absorption

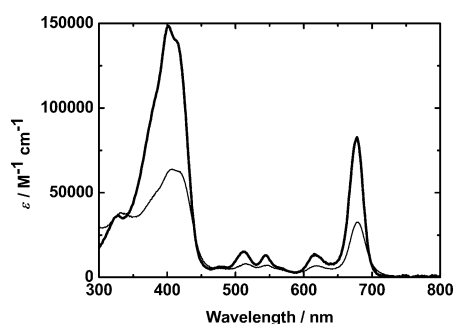


Figure 3. Absorption spectra of **2** (thin solid line) and **1** (bold solid line) in toluene.

spectrum reveals maxima at 324, 418, 511, 540, 614, and 671 nm (Figure S39, Supporting Information). For chlorin dimer–azafulleroid **2**, absorptions are observed in toluene at 334, 407, 514, 545, 618, and 679 nm (Figure 3), whereas in ben-

zonitrile, the corresponding absorptions are maximized at 329, 418, 512, 542, 613, and 671 nm (Figure S40, Supporting Information). Similarly to what is seen for **4**, the absorption spectra of the electron donor–acceptor conjugate **2** in toluene and benzonitrile are best described as the superimpositions of the chlorin dimer absorption of **1** and that of benzyl azafulleroid **5**.

Notably, the observed dependence between the solvent polarity and absorption spectra in any of the chlorin-dimer-containing systems **1** and **2** is similar to that observed previously in similar systems,^[11] and stems from intramolecular hydrogen bonding and π – π interactions between partly overlapping chlorins in nonpolar solvents.

Insights into electron donor–acceptor interactions have come from fluorescence assays. Chlorin monomer **3** exhibits strong fluorescence in the range 620–800 nm, with a fluorescence maximum at 676 nm (Figure 4), a fluorescence quantum

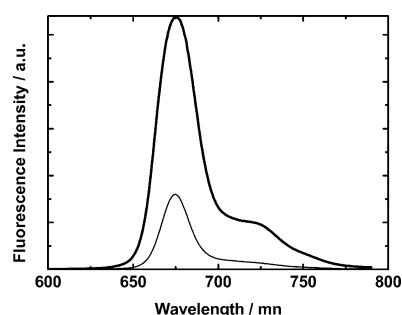


Figure 4. Fluorescence spectra of **4** (thin solid line) and reference **3** (bold solid line) in toluene upon photoexcitation at 403 nm.

yield of 0.2 in toluene, and a fluorescence lifetime of 6.7 ns (Figure S41, Supporting Information). In the case of **4**, the general shape of the fluorescence spectrum is practically identical to that observed for **3** (Figure 4). However, the chlorin fluorescence quantum yield is quenched, with values ranging from 0.029 in toluene to 0.034 in benzonitrile (Table 1).

Regarding the chlorin dimer reference, **1** exhibits strong fluorescence in the range 600–800 nm, with a fluorescence maximum at 684 nm, a fluorescence quantum yield of 0.27 in toluene, and a fluorescence lifetime of 6.0 ns (Figure S41, Supporting Information). Molecule **2** shows, in general, the same chlorin-dimer-centered fluorescence (Figure 5), but the fluorescence quantum yields are quenched with values ranging from 0.075 in toluene to 0.083 in benzonitrile (Table 1).

Our observation, namely that the fluorescence in **2** and **4** is nearly quantitatively quenched, points to an additional decay mechanism, that is, electron or energy transfer, of the chlorin or chlorin-dimer-centered singlet excited states. Again, evidence for intramolecular hydrogen bonding is obtained from the fluorescence spectra as the maxima of chlorin dimers **1** and **2** appear in toluene at longer wavelengths than those of chlorin monomers **3** and **4**. In polar benzonitrile, **1**, **2**, **3**, and **4** feature fluorescence maxima at 676 nm.

Transient absorption spectroscopy based on femtosecond and nanosecond pump–probe experiments shed light on the notion of an electron-transfer deactivation. For **3**, the singlet

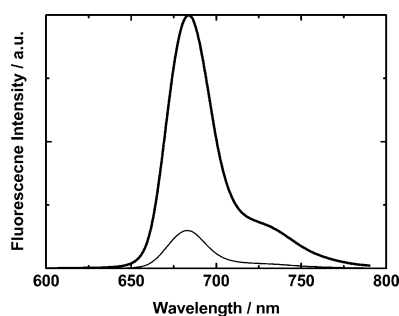


Figure 5. Fluorescence spectra of **2** (thin solid line) and reference **1** (bold solid line) in toluene upon photoexcitation at 403 nm.

Table 1. Summary of the photophysical properties.

	Fluorescence quantum yield	First excited singlet state lifetime	Singlet oxygen quantum yield	Charge-separated state lifetime [ps]
1 in toluene	0.27	6.0 ± 0.6 ns ^[a]	0.70	–
2 in <i>o</i> -xylene	0.070	74 ± 9.0 ps	^[b]	1622 ± 87
2 in toluene	0.095	12 ± 1.0 ps	0.99	1606 ± 46
2 in anisole	0.083	2.7 ± 1.6 ps	^[b]	283 ± 15
2 in THF	0.072	2.0 ± 1.0 ps	^[b]	68 ± 3
2 in benzonitrile	0.066	3.5 ± 1.0 ps	0.23	73 ± 4
2 in DMF	0.063	0.8 ± 0.8 ps	^[b]	21 ± 1
3 in toluene	0.20	6.7 ± 0.7 ns ^[a]	0.76	–
4 in <i>o</i> -xylene	^[b]	111 ± 10 ps	^[b]	907 ± 20
4 in toluene	0.029	103 ± 7 ps	0.74	830 ± 17
4 in anisole	0.031	37 ± 3 ps	^[b]	301 ± 9
4 in THF	0.050	6 ± 1 ps	^[b]	66 ± 4
4 in benzonitrile	0.034	1 ± 1 ps	0.19	65 ± 3
4 in DMF	0.038	0.6 ± 0.3 ps	^[b]	21 ± 1

[a] Determined from the fluorescence lifetime measurements. [b] Not determined.

excited state is formed immediately after the laser pulse, revealing a broad transient absorption with maxima at 490, 530, 580, 625, and 1100 nm, accompanied by minima at 515, 540, and 620 nm mirroring the ground-state absorption (Figure S43, Supporting Information). This transient absorption decays with a lifetime of 6.8 ns into the triplet manifold with transient maxima at 320, 460, and 560 nm and transient minima at 400 and 660 nm (Figure S44, Supporting Information).

In **4**, the same transient absorption features were observed. For example, immediately after the laser pulse, the chlorin-based singlet excited state is seen, which decays rapidly (Figure 6). The decay of the singlet excited state gives rise to a new set of transient absorption maxima at 460, 530, 585, 790, and 1050 nm as well as transient absorption minima at 510 and 540 nm (Figure 6). The transient absorption maxima at 460, 530, 585, and 790 nm are attributed to the chlorin radical cation, whereas the transient absorption at 1050 nm matches the absorption of the azafulleroid radical anion. In other words, the transient absorption spectrum provides evidence for the successful formation of a charge-separated state. By following the time evolution of the charge-separated state char-

acteristics, we derived lifetimes between 907 ± 20 ps (*o*-xylene) and 21 ± 1 ps (DMF) (Table 1). As far as the product of charge recombination is concerned, transient absorption measurements based on nanosecond laser photolysis (Figure S45, Supporting Information) and singlet oxygen phosphorescence studies (Table 1) corroborate that the triplet excited state evolves in nonpolar solvents. In contrast, deactivation to the ground state is the main channel in polar solvents.

Concerning chlorin dimer **1**, the singlet first excited state is formed immediately after the laser pulse, showing a transient absorption with maxima at 490, 535, 595, 635, and 1100 nm as well as minima at 520 and 550 nm (Figure S42, Supporting Information). With a lifetime of 6.0 ns, this transient absorption transforms into the triplet manifold featuring maxima at 300, 490, and 600 nm as well as minima at 400 and 680 nm (Figure S46, Supporting Information).

Similarly to **1**, **2** features the chlorin-dimer-based singlet excited state. The latter decays rapidly and is replaced by a new set of transient absorptions, including maxima at 465, 530, 595, 635, 790, and 1050 nm (Figure 7). The transient absorption maximum around 1050 nm is attributed to the absorption of the azafulleroid radical anion, whereas the remaining transient absorptions are attributed to the chlorin dimer radical cation.^[5c] Our assumption regarding the features of the chlorin dimer radical cation was further corroborated by pulse radiolysis assays (Figure S48, Supporting Information). As such, the transient absorption of the radiolysis-induced oxidation of **1** matches well the transient absorption of the chlorin dimer radical cation formed upon photoinduced oxidation in **2**. Particularly diagnostic for the chlorin dimer radical cation is the transient absorption maximizing around 790 nm, where neither the singlet excited nor triplet excited state of the chlorin dimer shows strong transient absorption bands.

The transient absorption changes caused by the charge-separated state were taken to determine the underlying lifetimes, which range from 1622 ± 87 ps (*o*-xylene) to 21 ± 1 ps (DMF; Table 1).

Singlet oxygen phosphorescence (Table 1) and nanosecond transient absorption measurements (Figure S47, Supporting Information) were employed to clarify the mechanism of charge recombination. In polar solvents, the charge-separated state reinstates directly the ground state, whereas in nonpolar solvents, the chlorin-dimer-centered triplet excited state evolves with maxima at 300, 420, 500, and 600 nm as well as minima at 400, 440, and 680 nm. Please note, however, that we have no particular evidence for the formation of any azafulleroid triplet excited state with its characteristic absorptions at 450 and 710 nm (Figure S49, Supporting Information).

Electrochemical studies

We performed differential pulse voltammetry (DPV) experiments in benzonitrile to gather information about any of the

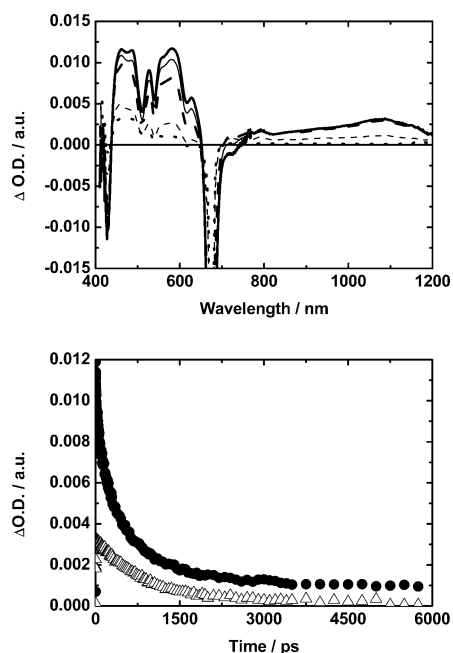


Figure 6. Top: Femtosecond transient absorption spectra of **4** in argon-saturated toluene; 1 ps (bold line), 10 ps (thin line), 100 ps (bold dashed line), 1000 ps (thin dashed line), and 5500 ps (dotted line) after excitation at 675 nm. Bottom: Corresponding absorption time profiles at 590 nm (filled circles) and 1050 nm (open triangles).

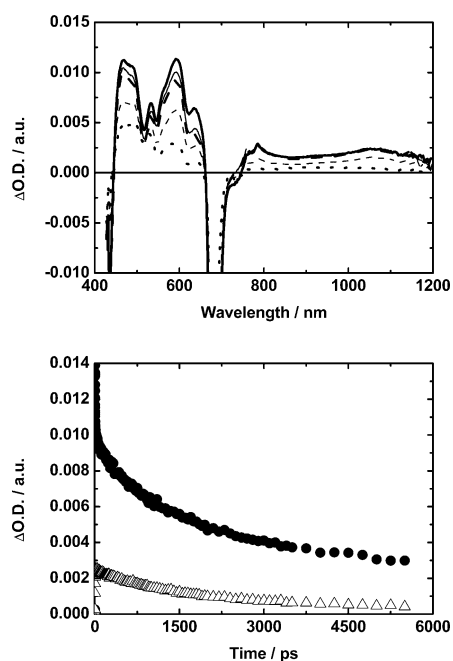


Figure 7. Top: Femtosecond transient absorption spectra of **2** in argon-saturated toluene; 1 ps (bold line), 10 ps (thin line), 100 ps (bold dashed line), 1000 ps (thin dashed line), and 5500 ps (dotted line) after excitation at 675 nm. Bottom: Corresponding absorption time profiles at 590 nm (filled circles) and 1050 nm (open triangles).

redox reactions occurring. All values are relative to a Fc/Fc^+ internal reference. As such, all compounds show amphoteric redox behavior with oxidative and reductive processes (Table S1, Supporting Information), with the exception of

benzyl azafulleroid **5**. The latter shows only three reductions at -0.33 , -0.76 , and -1.25 V. On one hand, **1** and **3** display one oxidation at $+0.94$ and $+0.89$ V, respectively, and two reductions, at -0.99 and -1.36 V in **1**, and at -1.06 and -1.31 V in **3**. On the other hand, in **2**, chlorin-centered oxidation appears at $+0.98$ V with reductions at -0.99 and -1.36 V, whereas the azafulleroid-centered reductions appear at -0.33 , -0.78 , and -1.18 V. In **4**, Chl-centered oxidation appears at $+1.03$ V and Chl-centered reductions at -0.95 and -1.27 V. In addition, azafulleroid-centered reductions are observed at -0.33 , -0.66 , and -1.13 V. Calculations of the differences between the one-electron oxidation and one-electron reduction lead to estimations of the HOMO–LUMO gaps of 1.93, 1.31, 1.95, and 1.36 V for **1**, **2**, **3**, and **4**, respectively.

Theoretical calculations

In order to elucidate the origin of the charge-separated state lifetimes, we performed computational studies at the DFT level using TPSS-D3/def2-SVP.^[26] In our previous supramolecular chlorin- C_{60} study we showed that the chosen computational method and level provide geometries and MOs that were appropriate for rationalizing the experimental phenomena.^[5k] Specifically, the chlorin- C_{60} center-to-center distances as well as the solvent polarity were found to be crucial for rationalizing the charge recombination dynamics.

In the present study, the charge-separated state lifetime of the chlorin monomer–azafulleroid **4** and chlorin dimer–azafulleroid **2** are affected significantly by the solvent polarity. In general, longer charge-separated state lifetimes are observed in less polar media (Table 1). As such, **2** and **4** exhibit similarly short lifetimes in polar solvents, whereas in nonpolar media their lifetimes differ significantly, with the lifetime of **2** nearly twice that observed for **4**. These observations contrast with the usual media effect, namely, that polar solvents stabilize charged molecular species, and, in turn, lead to longer charge-separated state lifetimes. Therefore, we assume that the folding and the specific molecular conformations play an important role in the charge separation events. With respect to the NMR studies performed with **2**, in nonpolar media, the hydrogen-bonding interactions stabilize the folded chlorin dimer conformation **A**, whereas an increase in solvent polarity forces the dimer moiety into open conformations.

In the quest for energy minima conformations, two extreme geometries were found (Figures 8 and S50): **A**, in which the chlorins are folded by the hydrogen bonds, and **B**, wherein the chlorins wrap an azafulleroid. Computational free-energy values, ΔG (298.15 K), indicated that, upon application of either toluene or benzonitrile implicit solvent models, the wrapped conformation **B** would be more stable than the folded one by 12 or 13 kcal mol^{-1} , respectively (Table S2). In general, the incomplete computational accuracy in the ΔG predictions, especially in toluene, probably arises because no real solvent molecules or dynamics were included, and solute–solvent coordinative and especially π – π -stacking interactions are missing. As a result, the chlorin–azafulleroid π – π -stacking interactions are overestimated if the competing solvent interactions

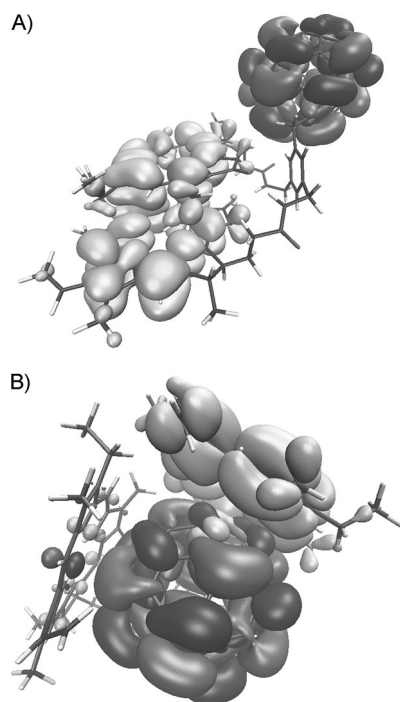


Figure 8. TPSS-D3/def2-SVP geometry-optimized conformers and frontier MOs for chlorin dimer-azafulleroid **2** in solution. HOMO (light) and LUMO (dark) MOs for **A**: chlorin-folded conformation ($\Delta = 0.95$ eV) and for **B**: C_{60} -wrapped conformation ($\Delta = 1.12$ eV), calculated in toluene and benzonitrile, respectively. Isosurface value 0.01.

are not implemented. Nevertheless, despite the lack of direct experimental evidence, the wrapped conformation is the most likely geometry in benzonitrile. An additional notion for this hypothesis comes from the fact that various porphyrin dimers have been reported to host C_{60} .^[27] Furthermore, the interaction in the wrapped conformation is considered to be hydrophobic. In other words, it is more stabilized in polar solvents, corresponding to the $\Delta\Delta G(\mathbf{B}-\mathbf{A})$ values between the studied solvents and experimental data. We consider that despite the deficiency in the ΔG values, the geometries are still relevant for describing possible extreme conformations.

Inspection of the frontier orbitals (Figure 8) reveals that in the **A** and **B** conformers, the HOMO is located on the electron-donating chlorin, whereas the LUMO is centered on the electron-accepting azafulleroid. Notably, in the folded structure **A**, the HOMO is delocalized evenly and also partly shared between chlorins, which leads to stabilization of the radical cation and, in turn, to an increase in the charge-separated state lifetime. In contrast, in the wrapped conformation **B** present in polar solvents, the radical cation cannot be stabilized by the delocalization. Nevertheless, according to the Marcus theory of electron transfer, the charge-separated-state lifetime depends strongly on the solvent polarity^[28] (that is, as the solvent polarity decreases, the charge-recombination dynamics are pushed deeper into the Marcus inverted region) and on the distance between the electron donor and acceptor.^[29] In the present study, the wrapped conformer **B** displays a significantly shorter center-to-center distance than the folded struc-

ture **A**. This may be the most critical parameter for explaining the differences in the observed lifetimes, as the charge-separated state lifetime of **4** is increased by a factor of approximately 40 upon going from polar to nonpolar solvents. Still, this comparison excludes the effect of hydrogen bonds, which is seen to increase the charge-separated state lifetime by a factor of two.

Overall, the effect of hydrogen bonds on the charge-separated state lifetime is seen from a comparison between **2** and **4** in two different nonpolar solvents, that is, toluene and *o*-xylene. With increasing polarity, the hydrogen bonds in the dimer structure open up, leading to a charge-separated state lifetime similar to that seen in the monomer. The rapid decrease in strongly polar solvents is explained by the favoring of the wrapped conformer **B**, which features short center-to-center distances, and, hence, destabilized charge-separated states.

Finally, the structures of **1** and **2** and their folded geometries bear little resemblance to the pairs in photosynthetic reaction centers such as *Rhodospseudomonas viridis* (Scheme 1). First of all, in the current model the chlorins are metal-free, whereas in natural systems, Mg is coordinated. Secondly, the folded conformations have partial π - π overlap between C rings, whereas the natural systems exhibit precise ring overlapping in ring A (Schemes 1 and 2). Moreover, the Q_y transition dipole moment vectors are oriented at a 35° angle, whereas in the natural systems, the optimal angle of the Q_y vectors is 180° . Also, upon comparison of our models with classic SP models,^[9a-e,10] the features mentioned above are, in most cases, more accurately imitated in the latter ones. However, from a functional point of view, the charge-separated state lifetime in **2** mimics qualitatively that of the original SP. Furthermore, the strength of our models lies in its simplicity, that is, the C_2 -symmetry dimer folding is based purely on intramolecular processes, without the need for external bridging units such as H_2O , and, thus, is entropically favored. The chlorin complexes are also chemically stable, and in nonpolar media, the folded geometry is highly populated even at room temperature.

Conclusions

To summarize, we have described the synthesis and characterization of chlorin monomer-azafulleroid **4** and chlorin dimer-azafulleroid **2**. Their photophysical properties were studied with particular emphasis on solvent-induced conformational changes. To this end, in nonpolar media, **2** presents a folded conformation, as confirmed by UV/Vis, fluorescence, and NMR spectroscopies. The folding is unequivocally favored entropically, because the *m*-xylene linkage brings the chlorins into close proximity. Here, intramolecular folding occurs without the need for crosslinking bridges, which are frequently found in biomimetic SP dimers.

Advanced photophysical techniques such as transient absorption spectroscopy provided unambiguous evidence for the successful formation of the charge-separated state, which decays more slowly in **2** than in the corresponding reference **4**, regardless of solvent polarity. Moreover, **2** exhibits C_2 sym-

metry in nonpolar media, which leads to a long-lived charge-separated state, whereas in polar media, the charge-separated state has a shorter lifetime.

Complementary DFT calculations corroborated the existence of two different energy minimum conformations, namely a folded one in nonpolar media and a wrapped one in polar media.

As was pursued in the synthetic and conformational design, the folded conformer of **2** features functional similarities with the SP found in photosynthetic reaction centers, even though it is structurally far from the complexity of natural systems. In this context, our next challenge is to develop a folding strategy that addresses, for instance, the use of synthetic tools to adjust the geometry, to incorporate metal ligands, and to use auxiliary chlorins to facilitate and mediate charge transfer.

Experimental Section

The synthesis and characterization of all compounds are described in detail in the Supporting Information. The NMR spectra including ^1H , ^{13}C , COSY, NOESY, HSQC, and HMBC are presented in Figures S1–S36 in the Supporting Information.

Absorption and emission spectroscopy

Steady-state UV/Vis absorption spectra were measured on Cary5000 (Varian) and PerkinElmer Lambda 2 two-beam spectrophotometers. Steady-state fluorescence spectra were taken from samples with a FluoroMax3 spectrometer (Horiba Jobin Yvon). The experiments were performed at room temperature. Fluorescence quantum yields were determined by the comparative method^[30,31] using H_2TPP and ZnTPP as references with fluorescence quantum yields of 0.11 and 0.03, respectively, in toluene. Singlet oxygen phosphorescence measurements were conducted using a Fluorolog 3 (Horiba Jobin Yvon) equipped with an IGA Symphony ($512 \times 1 \times 1 \mu\text{m}$) detector (Horiba Jobin Yvon). The singlet oxygen phosphorescence quantum yields were determined by the comparative method, employing H_2TPP and ZnTPP as references with singlet oxygen quantum yields of 0.66 and 0.72, respectively, in toluene.^[32]

Time-resolved fluorescence studies

Fluorescence lifetimes were determined through the time-correlated single photon counting (TCSPC) technique using a Fluorolog 3 (Horiba Jobin Yvon). The sample was excited with a NanoLED-405 instrument (403 nm), and the signal was detected by a Hamamatsu MCP photomultiplier (type R3809U-50). The time profiles were recorded at 680 nm.

Transient absorption spectroscopy

Transient absorption measurements based on femtosecond laser photolysis were performed with output from a Ti/sapphire laser system (CPA2110, Clark-MXR Inc.): 775 nm, 1 kHz, and 150 fs FWHM pulses. The excitation wavelength was generated either by second harmonic generation (387 nm) or by using a non-collinear optical parametric amplifier (NOPA Pulse, Clark MXR) (675 nm). For both excitation wavelengths, pulse widths of < 150 fs and energies of 200 nJ/pulse (387 nm) and 120 nJ/pulse (675 nm) were selected. The transient absorption detection was performed with a transient absorption pump/probe system (TAPPS, Ultrafast Systems).

Nanosecond transient absorption laser photolysis measurements were performed with the output from an optical parametric oscillator (OPO, Rainbow VIR, Opotek/Quantel, output: 420 nm, 10 mJ/pulse) pumped by the third harmonic (355 nm) of a Nd:YAG laser (Brilliant, Quantel). The optical detection was based on a pulsed (pulser MSP 05, Müller Elektronik-Optik) xenon lamp (XBO 450, Osram), a monochromator (Spectra Pro 2300i, Acton Research), a R928 photomultiplier tube (Hamamatsu Photonics), or a fast InGaAs photodiode (Nano 5, Coherent) with 300 MHz amplification, and a 1 GHz digital oscilloscope (WavePro7100, LeCroy).

Pulse radiolysis

The samples were dissolved in CHCl_3 , saturated with O_2 , and irradiated with high-energy electron pulses (1 MeV, 15 ns duration) by a pulse-transformer-type electron accelerator (Elit, Institute of Nuclear Physics, Novosibirsk, Russia). The dose delivered per pulse was measured by electron dosimetry. Doses of 100 Gy/pulse were employed. Optical detection of the transients was performed with a detection system consisting of a pulsed (pulser MSP 05, Müller Elektronik Optik) xenon lamp (XBO 450, Osram), a SpectraPro 500 monochromator (Acton Research Corporation), a R9220 photomultiplier (Hamamatsu Photonics), and a 500 MHz digitizing oscilloscope (TDS 640, Tektronix). A more detailed description of the overall setup is reported elsewhere.^[33]

Electrochemical studies

Electrochemical experiments were performed with a Metrohm FRA 2 $\mu\text{Autolab}$ Type III potentiostat, in benzonitrile containing 0.1 M TBAPF₆ as the supporting electrolyte. A single-compartment, three-electrode cell configuration was used in this work. A glassy carbon electrode (3 mm diameter) was used as the working electrode, a Pt wire as the counter electrode, and a Ag wire as the reference electrode. All potentials were corrected against the Fc/Fc^+ internal reference.

Computational methods

Full computational details, including Cartesian coordinates of all studied structures, are given in the Supporting Information.

Acknowledgements

Dr. Petri Heinonen is gratefully accredited for the HRMS measurements. M.Sc. Valtteri Mäkelä and Dr. Sami Heikkinen are acknowledged for their assistance in the NMR measurements. Funding was received from the Academy of Finland (project No 129062). M.Sc. Taru Nikkonen acknowledges the Marie Curie Initial Training Network FUNMOLS, the Graduate School of Organic Chemistry and Chemical Biology (GSOCCB), and the Finnish Cultural Foundation for financial support. Dr. María Moreno Oliva acknowledges financial support from the Marie Curie COFUND programme “U-Mobility”, cofinanced by Universidad de Malaga and the European Community’s Seventh Framework Programme under Grant Agreement No. 246550. Dr. Axel Kahnt gratefully acknowledges funding from the Deutsche Forschungsgemeinschaft (DFG) through grant KA 3491/2-1. Funding from the Bayerische Staatsregierung as part of the “Solar Technologies go Hybrid” initiative is gratefully acknowledged. We would like to thank Prof. Abel and his group from

Leipzig University, Leipzig, Germany, for support during the pulse radiolysis measurements. The Finnish National Centre for Scientific Computing (CSC) is recognized for computational resources.

Keywords: chlorophyll • conformational switching • photoinduced charge separation • photosynthesis • special pair

- [1] H. Scheer in *Chlorophylls and Bacteriochlorophylls: Biochemistry Biophysics, Functions and Applications. Advances in Photosynthesis and Respiration*, Vol. 25 (Eds.: B. Grimm, R. J. Porra, W. Rüdiger, H. Scheer), Springer, Dordrecht, **2006**, pp. 1–26.
- [2] T. S. Balaban, *Acc. Chem. Res.* **2005**, *38*, 612–623.
- [3] a) J. J. Katz, J. C. Hindman in *Photochemical Conversion and Storage of Solar Energy* (Ed.: J. S. Connolly), Academic Press, London, **1981**, pp. 27–78; b) J. J. Katz, J. R. Norris, L. L. Shipman, M. C. Thurnauer, M. R. Wasielewski, *Annu. Rev. Biophys. Bioeng.* **1978**, *7*, 393–434.
- [4] a) Protein Data Bank identification code, PDB ID code = 1PRC; b) Accelrys Software Inc., Discovery Studio Modeling Environment, Release 4.0, San Diego, Accelrys Software, **2013**.
- [5] a) S. Fukuzumi, K. Ohkubo, Y. Chen, R. K. Pandey, R. Zhan, J. Shao, K. M. Kadish, *J. Phys. Chem. A* **2002**, *106*, 5105–5113; b) S. Fukuzumi, K. Ohkubo, H. Imahori, J. Shao, Z. Ou, G. Zheng, Y. Chen, R. K. Pandey, M. Fujitsuka, O. Ito, K. M. Kadish, *J. Am. Chem. Soc.* **2001**, *123*, 10676–10683; c) A. R. Holzwarth, M. Katterle, M. G. Müller, Y.-Z. Ma, V. Prokhorenko, *Pure Appl. Chem.* **2001**, *73*, 469–474; d) J. S. Kavakka, S. Heikkinen, I. Kilpeläinen, M. Mattila, H. Lipsanen, J. Helaja, *Chem. Commun.* **2007**, 519–521; e) J. S. Kavakka, S. Heikkinen, I. Kilpeläinen, N. V. Tkachenko, J. Helaja, *Chem. Commun.* **2009**, 758–760; f) F.-P. Montforts, O. Kutzki, *Angew. Chem.* **2000**, *112*, 612–614; *Angew. Chem. Int. Ed.* **2000**, *39*, 599–601; g) K. Ohkubo, H. Kotani, J. Shao, Z. Ou, K. M. Kadish, G. Li, R. K. Pandey, M. Fujitsuka, O. Ito, H. Imahori, S. Fukuzumi, *Angew. Chem.* **2004**, *116*, 871–874; *Angew. Chem. Int. Ed.* **2004**, *43*, 853–856; h) N. V. Tkachenko, L. Rantala, A. Y. Tauber, J. Helaja, P. H. Hynninen, H. Lemmetyinen, *J. Am. Chem. Soc.* **1999**, *121*, 9378–9387; i) M. R. Wasielewski, G. P. Wiederrecht, W. A. Svec, M. P. Niemczyk, *Sol. Energy Mater. Sol. Cells* **1995**, *38*, 127–134; j) V. Vehmanen, N. V. Tkachenko, A. Y. Tauber, P. H. Hynninen, H. Lemmetyinen, *Chem. Phys. Lett.* **2001**, *345*, 213–218; k) K. Stranius, V. Iashin, T. Nikkonen, M. Muuronen, J. Helaja, N. Tkachenko, *J. Phys. Chem. A* **2014**, *118*, 1420–1429.
- [6] a) B. Grimm, A. Hausmann, A. Kahnt, W. Seitz, F. Spänig, D. M. Guldi in *Handbook of Porphyrin Science* (Eds.: K. M. Kadish, K. M. Smith, R. Guillard), World Scientific Publishing, **2010**, *1*, 133–219; b) F. D'Souza, O. Ito, *Coord. Chem. Rev.* **2005**, *249*, 1410–1422; c) M. E. El-Khouly, O. Ito, P. M. Smith, F. D'Souza, *J. Photochem. Photobiol. C* **2004**, *5*, 79–104; d) F. D'Souza, S. Gadde, D.-M. S. Islam, C. A. Wijesinghe, A. L. Schumacher, M. E. Zandler, Y. Araki, O. Ito, *J. Phys. Chem. A* **2007**, *111*, 8552–8560; e) C. Ehli, G. M. Aminur Rahman, N. Jux, D. Balbinot, D. M. Guldi, F. Paolucci, M. Marcaccio, D. Paolucci, M. Melle-Franco, F. Zerbetto, S. Campidelli, M. Prato, *J. Am. Chem. Soc.* **2006**, *128*, 11222–11231; f) F. D'Souza, P. M. Smith, M. E. Zandler, A. L. McCarty, M. Ito, Y. Araki, O. Ito, *J. Am. Chem. Soc.* **2004**, *126*, 7898–7907; g) D. M. Guldi, *Pure Appl. Chem.* **2003**, *75*, 1069–1075; h) D. M. Guldi, *Chem. Soc. Rev.* **2002**, *31*, 22–36; i) D. M. Guldi, A. Hirsch, M. Scheloske, E. Dietel, A. Troisi, F. Zerbetto, M. Prato, *Chem. Eur. J.* **2003**, *9*, 4968–4979; j) J. Iehl, M. Vartanian, M. Holler, J.-F. Nierengarten, B. Delavaux-Nicot, J. M. Strub, A. Van Dorsseleer, Y. Wu, J. Mohanraj, K. Yoosaf, N. Armario, *J. Mater. Chem.* **2011**, *21*, 1562–1573; k) H. Imahori, *Org. Biomol. Chem.* **2004**, *2*, 1425–1433; l) H. Imahori, M. E. El-Khouly, M. Fujitsuka, O. Ito, Y. Sakata, S. Fukuzumi, *J. Phys. Chem. A* **2001**, *105*, 325–332; m) H. Imahori, D. M. Guldi, K. Tamaki, Y. Yoshida, C. Luo, Y. Sakata, S. Fukuzumi, *J. Am. Chem. Soc.* **2001**, *123*, 6617–6628; n) G. Kodis, P. A. Liddell, A. L. Moore, T. A. Moore, D. Gust, *J. Phys. Org. Chem.* **2004**, *17*, 724–734; o) D. Kuciauskas, S. Lin, G. R. Seely, A. L. Moore, T. A. Moore, D. Gust, T. Drovetskaya, C. A. Reed, P. D. W. Boyd, *J. Phys. Chem.* **1996**, *100*, 15926–15932; p) C. Luo, D. M. Guldi, H. Imahori, K. Tamaki, Y. Sakata, *J. Am. Chem. Soc.* **2000**, *122*, 6535–6551; q) E. Maligaspe, N. V. Tkachenko, N. K. Subbaiyan, R. Chitta, M. E. Zandler, H. Lemmetyinen, F. D'Souza, *J. Phys. Chem. A* **2009**, *113*, 8478–8489; r) T. Palacin, H. L. Khanh, B. Joussetme, P. Jegou, A. Filoramo, C. Ehli, D. M. Guldi, S. Campidelli, *J. Am. Chem. Soc.* **2009**, *131*, 15394–15402.
- [7] a) B. Ballesteros, S. Campidelli, G. de La Torre, C. Ehli, D. M. Guldi, M. Prato, T. Torres, *Chem. Commun.* **2007**, 2950–2952; b) B. Ballesteros, G. de La Torre, C. Ehli, G. M. Aminur Rahman, F. Agulló-Rueda, D. M. Guldi, T. Torres, *J. Am. Chem. Soc.* **2007**, *129*, 5061–5068; c) S. Campidelli, B. Ballesteros, A. Filoramo, D. Díaz Díaz, G. de La Torre, T. Torres, G. M. Aminur Rahman, C. Ehli, D. Kiessling, F. Werner, V. Sgobba, D. M. Guldi, C. Cioffi, M. Prato, J.-P. Bourgoïn, *J. Am. Chem. Soc.* **2008**, *130*, 11503–11509; d) U. Hahn, S. Engmann, C. Oelsner, C. Ehli, D. M. Guldi, T. Torres, *J. Am. Chem. Soc.* **2010**, *132*, 6392–6401; e) M. Ince, M. Martínez-Díaz, J. Barberá, T. Torres, *J. Mater. Chem.* **2011**, *21*, 1531–1536; f) H. Lemmetyinen, T. Kumpulainen, M. Niemi, A. Efimov, J. Ranta, K. Stranius, N. V. Tkachenko, *Photochem. Photobiol. Sci.* **2010**, *9*, 949–959; g) H. Neugebauer, M. A. Loi, C. Winder, N. Serdar Sariciftci, G. Cerullo, A. Gouloumis, P. Vázquez, T. Torres, *Sol. Energy Mater. Sol. Cells* **2004**, *83*, 201–209; h) M. Niemi, N. V. Tkachenko, A. Efimov, H. Lehtivuori, K. Ohkubo, S. Fukuzumi, H. Lemmetyinen, *J. Phys. Chem. A* **2008**, *112*, 6884–6892; i) M. S. Rodríguez-Morgade, M. E. Plonska-Brzezinska, A. J. Athans, E. Carbonell, G. de Miguel, D. M. Guldi, L. Echegoyen, T. Torres, *J. Am. Chem. Soc.* **2009**, *131*, 10484–10496; j) G. Rotas, J. Ranta, A. Efimov, M. Niemi, H. Lemmetyinen, N. Tkachenko, N. Tagmatarchis, *ChemPhysChem* **2012**, *13*, 1246–1254; k) W. Seitz, A. Kahnt, D. M. Guldi, T. Torres, *J. Porphyrins Phthalocyanines* **2009**, *13*, 1034–1039; l) T. Torres, A. Gouloumis, D. Sanchez-Garcia, J. Jayawickramarajah, W. Seitz, D. M. Guldi, J. L. Sessler, *Chem. Commun.* **2007**, 292–294.
- [8] a) F. D'Souza, E. Maligaspe, K. Ohkubo, M. E. Zandler, N. K. Subbaiyan, S. Fukuzumi, *J. Am. Chem. Soc.* **2009**, *131*, 8787–8797; b) F. D'Souza, R. Chitta, S. Gadde, L. M. Rogers, P. A. Karr, M. E. Zandler, A. S. D. Sandanayaka, Y. Araki, O. Ito, *Chem. Eur. J.* **2007**, *13*, 916–922; c) A. S. D. Sandanayaka, N. K. Subbaiyan, R. Chitta, Y. Araki, O. Ito, F. D'Souza, *J. Porphyrins Phthalocyanines* **2008**, *12*, 857–865; d) M. A. Filatov, F. Laquai, D. Fortin, R. Guillard, P. D. Harvey, *Chem. Commun.* **2010**, *46*, 9176–9178; e) M. Isosomppi, N. V. Tkachenko, A. Efimov, H. Lemmetyinen, *J. Phys. Chem. A* **2005**, *109*, 4881–4890; f) M. Morisue, D. Kalita, N. Haruta, Y. Kobuke, *Chem. Commun.* **2007**, 2348–2350; g) A. Osuka, S. Nakajima, K. Maruyama, N. Mataga, T. Asahi, I. Yamazaki, Y. Nishimura, T. Ohno, K. Nozaki, *J. Am. Chem. Soc.* **1993**, *115*, 4577–4589; h) H. Ozeki, A. Nomoto, K. Ogawa, Y. Kobuke, M. Murakami, K. Hosoda, M. Ohtani, S. Nakashima, H. Miyasaka, T. Okada, *Chem. Eur. J.* **2004**, *10*, 6393–6401; i) J. Rodriguez, C. Kirmaier, M. R. Johnson, R. A. Friesner, D. Holten, J. L. Sessler, *J. Am. Chem. Soc.* **1991**, *113*, 1652–1659; j) J. L. Sessler, M. R. Johnson, T.-Y. Lin, S. E. Creager, *J. Am. Chem. Soc.* **1988**, *110*, 3659–3661; k) F. Brégier, S. M. Aly, C. P. Gros, J. M. Barbe, Y. Roussel, P. D. Harvey, *Chem. Eur. J.* **2011**, *17*, 14643–14662.
- [9] a) M. R. Wasielewski, M. H. Studier, J. J. Katz, *Proc. Natl. Acad. Sci. USA* **1976**, *73*, 4282–4286; b) S. G. Boxer, G. L. Closs, *J. Am. Chem. Soc.* **1976**, *98*, 5406–5408; c) M. R. Wasielewski, W. A. Svec, *J. Org. Chem.* **1980**, *45*, 1969–1974; d) R. R. Bucks, S. G. Boxer, *J. Am. Chem. Soc.* **1982**, *104*, 340–343; e) H. Tamiaki, K. Fukai, H. Shimazu, K. Nishide, Y. Shibata, S. Itoh, M. Kunieda, *Photochem. Photobiol. Sci.* **2008**, *7*, 1231–1237; f) D. G. Johnson, W. A. Svec, M. R. Wasielewski, *Isr. J. Chem.* **1988**, *28*, 193–203; g) A. Osuka, S. Marumo, Y. Wada, I. Yamazaki, T. Yamazaki, Y. Shirakawa, Y. Nishimura, *Bull. Chem. Soc. Jpn.* **1995**, *68*, 2909–2915; h) S. Shinoda, A. Osuka, *Tetrahedron Lett.* **1996**, *37*, 4945–4948; i) A. Osuka, Y. Wada, S. Shinoda, *Tetrahedron* **1996**, *52*, 4311–4326; j) N. Kosaka, H. Tamiaki, *Eur. J. Org. Chem.* **2004**, 2325–2330; k) M. R. Wasielewski, W. A. Svec, B. T. Cope, *J. Am. Chem. Soc.* **1978**, *100*, 1961–1962.
- [10] a) M. J. Pellin, K. J. Kaufmann, M. R. Wasielewski, *Nature* **1979**, *278*, 54–55; b) S. G. Boxer, R. R. Bucks, *J. Am. Chem. Soc.* **1979**, *101*, 1883–1885; c) R. R. Bucks, T. L. Netzell, I. Fujita, S. G. Boxer, *J. Phys. Chem.* **1982**, *86*, 1947–1955.
- [11] T. Nikkonen, R. Haavikko, J. Helaja, *Org. Biomol. Chem.* **2009**, *7*, 2046–2052.
- [12] M. P. Castaldi, S. E. Gibson, M. Rudd, A. J. P. White, *Chem. Eur. J.* **2006**, *12*, 138–148.
- [13] E. Diez-Barra, J. C. García-Martínez, S. Merino, R. del Rey, J. Rodríguez-López, P. Sánchez-Verdú, J. Tejada, *J. Org. Chem.* **2001**, *66*, 5664–5670.
- [14] S. González, N. Martín, A. Swartz, D. M. Guldi, *Org. Lett.* **2003**, *5*, 557–560.

- [15] L. Ulmer, J. Mattay, *Eur. J. Org. Chem.* **2003**, 2933–2940.
- [16] H. Hachiya, T. Kakuta, M. Takami, Y. Kabe, *J. Organomet. Chem.* **2009**, *694*, 630–636.
- [17] C. Yang, S. Cho, A. J. Heeger, F. Wudl, *Angew. Chem.* **2009**, *121*, 1620–1623; *Angew. Chem. Int. Ed.* **2009**, *48*, 1592–1595.
- [18] M. Cases, M. Duran, J. Mestres, N. Martin, M. Solà, *J. Org. Chem.* **2001**, *66*, 433–442.
- [19] T. Nakahodo, M. Okada, H. Morita, T. Yoshimura, M. O. Ishitsuka, T. Tsuchiya, Y. Maeda, H. Fujihara, T. Akasaka, X. Gao, S. Nagase, *Angew. Chem.* **2008**, *120*, 1318–1320; *Angew. Chem. Int. Ed.* **2008**, *47*, 1298–1300.
- [20] T. Grösser, M. Prato, V. Lucchini, A. Hirsch, F. Wudl, *Angew. Chem.* **1995**, *107*, 1462–1464; *Angew. Chem. Int. Ed. Engl.* **1995**, *34*, 1343–1345.
- [21] M. Prato, Q. Chan Li, F. Wuld, V. Lucchini, *J. Am. Chem. Soc.* **1993**, *115*, 1148–1150.
- [22] I. P. Romanova, O. A. Larionova, A. A. Balandina, Sh. K. Latypov, A. R. Mustafina, V. V. Skripacheva, V. V. Zverev, O. G. Sinyashin, *Russ. J. Gen. Chem.* **2008**, *78*, 451–456.
- [23] G. T. Pauly, N. A. Loktionova, Q. Fang, S. L. Vankayala, W. C. Guida, A. E. Pegg, *J. Med. Chem.* **2008**, *51*, 7144–7153.
- [24] J. Hummelen, C. Bellavia-Lund, F. Wudl in *Fullerenes and Related Structures*, Vol. 199 (Ed.: A. Hirsch), Springer/Berlin, Heidelberg, **1999**, pp. 93–134.
- [25] J. C. Hummelen, M. Prato, F. Wudl, *J. Am. Chem. Soc.* **1995**, *117*, 7003–7004.
- [26] See full list of computational references and details in the Supporting Information.
- [27] a) D. Sun, F. S. Tham, C. A. Reed, L. Chaker, M. Burgess, P. D. W. Boyd, *J. Am. Chem. Soc.* **2000**, *122*, 10704–10705; b) D. Sun, F. S. Tham, C. A. Reed, L. Chaker, P. D. W. Boyd, *J. Am. Chem. Soc.* **2002**, *124*, 6604–6612; c) K. Tashiro, T. Aida, J.-Y. Zheng, K. Kinbara, K. Saigo, S. Sakamoto, K. Yamaguchi, *J. Am. Chem. Soc.* **1999**, *121*, 9477–9478; d) J. Zheng, K. Tashiro, Y. Hirabayashi, K. Kinbara, K. Saigo, T. Aida, S. Sakamoto, K. Yamaguchi, *Angew. Chem.* **2001**, *113*, 1909–1913; *Angew. Chem. Int. Ed.* **2001**, *40*, 1857–1861.
- [28] a) R. A. Marcus, *J. Chem. Phys.* **1956**, *24*, 966–978; R. A. Marcus, *J. Chem. Phys.* **1957**, *26*, 867–871.
- [29] W. B. Davis, M. A. Ratner, M. R. Wasielewski, *J. Am. Chem. Soc.* **2001**, *123*, 7877–7886.
- [30] G. A. Crosby, J. N. Demas, *J. Phys. Chem.* **1971**, *75*, 991–1024.
- [31] P. G. Seybold, M. Gouterman, *J. Mol. Spectrosc.* **1969**, *31*, 1–13.
- [32] F. Wilkinson, W. P. Helman, A. B. Ross, *J. Phys. Chem. Ref. Data* **1993**, *22*, 113–262.
- [33] O. Brede, H. Orthner, V. Zubarev, R. Hermann, *J. Phys. Chem.* **1996**, *100*, 7097–7105.

Received: August 8, 2014

Published online on November 7, 2014